

Electronic Supplementary Information

BSA Stabilized Tetraphenylethylene Nanocrystals as Aggregation-Induced Enhanced Electrochemiluminescence Emitters for Ultrasensitive MicroRNA Assay

Jia-Li Liu, Ying Zhuo, Ya-Qin Chai,* Ruo Yuan*

*Key Laboratory of Luminescent and Real-Time Analytical Chemistry (Southwest University),
Ministry of Education, College of Chemistry and Chemical Engineering, Southwest University,
Chongqing 400715, China.*

* Corresponding authors at: Tel.: +86 23 68252277, fax: +86 23 68253172.

E-mail addresses: yqchai@swu.edu.cn (Y. Q. Chai), yuanruo@swu.edu.cn (R. Yuan)

* Corresponding authors at: Tel.: +86 23 68252277, fax: +86 23 68253172.

E-mail addresses: yqchai@swu.edu.cn (Y. Q. Chai), yuanruo@swu.edu.cn (R. Yuan).

Table of Contents

Electronic Supporting Information	S1
Experimental Section	S3
Reagents and Materials.....	S3
Table	
S1.....	S4
Cell Culture and Total RNA Extraction.....	S4
Apparatus.....	S4
Native Polyacrylamide Gel Electrophoresis	
(PAGE).....	S5
Preparation of the Sample Solution.....	S5
Fabrication of Biosensor.....	S5
Measurement Procedure.....	S6
Results and Discussion	S6
The Possible ECL Mechanisms.....	
S6	
ECL and EIS Characterization of the ECL Biosensing	
Platform.....	S7
Optimization of the Experimental Conditions.....	S8
The Sensitivity Analysis of the ECL Biosensing Platform	S9
Table S2.....	
S11	
Performance of the Proposed ECL Biosensing Platform.....	S11
The Method of LOD Calculation.....	S12
Application of the Biosensor in Tumor Cells.....	
S13	

Experimental Section

Reagents and Materials.

Tetraphenylethylene (TPE) was purchased from TCI Development Co., Ltd. (Shanghai, China). Triethylamine (TEA) was received from Kelong Chemical Inc. (Chengdu, China). Mono-(6-amino-6-deoxy)- β -cyclodextrin (NH_2 - β -CD), 1-(3-(Dimethylamino)propyl)-3-ethylcarbodiimide hydrochloride (EDC) and N-hydroxy succinimide (NHS) were purchased from Aladdin biochemical technology co. Ltd. (Shanghai, China). Bovine serum albumin (BSA, 96-99%) and glutaraldehyde (GA, 50%) were provided by Sigma-Aldrich Co. (St. Louis, MO, USA). BbvI and 10 \times CutSmart buffer were received from New England Biolabs Ltd. (Beverly, MA, USA). 10 \times CutSmart buffer contains 50 mM KAc, 20 mM Tris-Ac, 10 mM $\text{Mg}(\text{Ac})_2$, 100 $\mu\text{g}/\text{ml}$ BSA. The deionized water was purified by water purification system with an electrical resistance of $18.2 \text{ M}\Omega \cdot \text{cm}^{-1}$. The 1 \times TE buffer (10 mM Tris-HCl, 1.0 mM ethylenediamine tetraacetic acid (EDTA), pH 8.0) was employed to reserve DNA oligonucleotides. DNA/miRNA-141 hybridization buffer (10 mM Tris-HCl, 1.0 mM EDTA, 0.2 M NaCl, 10 mM MgCl_2 , pH 7.4), DNA hybridization buffer (10 mM Tris-HCl, 1.0 mM EDTA, 1.0 M NaCl, pH 7.4), and the phosphate buffered solutions (PBS), pH 7.4 (0.1 M Na_2HPO_4 , 0.1 M KH_2PO_4 and 0.1 M KCl, using 0.1 M HCl or 0.1 M NaOH solution to adjust pH) were used in this work. The nucleotide sequences of the oligonucleotides were list in Table S1.

Table S1. Sequence Information for the Nucleic Acids Used in This Study.

Name	Ssequences (5'-3')
Fc-H1	Fc-CGC CGG CAG CCC ATC TTT ACC AGA CAG TGT TAG CTG CCG GCG-Fc
Fc-H2	Fc-CGA GCT CGC CCG CCG GCA GCT AAC ACT GTC TGG TAA AGA TGG CGA GCT CG-Fc
miRNA-141	UAA CAC UGU CUG GUA AAG AUG G

Cell Culture and Total RNA Extraction.

The MDA-MB-231 cell line was obtained from the cell bank of the Committee on Type Culture Collection of Chinese Academy of Science (Shanghai, China) and cultured in DMEM containing 10% fetal bovine serum (FBS), 100 U/mL penicillin and 100 U/mL streptomycin, and maintained at 37 °C in a humidified 5% CO₂ incubator. Total RNA samples were extracted from cell line by using Trizol Reagent (TIANGEN Biotech (Beijing) Co., Ltd.) according to the manufacturer's protocol after cell counting.

Apparatus.

The scanning electron microscope (SEM) images of the materials were characterized by S-4800 scanning electron microscopy (Hitachi, Tokyo, Japan). The transmission electron microscope (TEM) images were obtained by JEM 1200EX TEM (JEOL Ltd, Tokyo, Japan). UV-vis absorption spectra were characterized by a UV-2450 UV-vis spectrophotometer (Shimadzu, Tokyo, Japan). Fluorescence spectra were characterized by FL-5700 spectrophotometer (Hitachi, Tokyo, Japan). The electrochemical measurements were performed on a CHI 660C electrochemistry workstation (Shanghai CH Instruments, China). ECL emission spectra were measured

on a Newton EMCCD spectroscopy detector (Andor Co., Tokyo, Japan) combined with an electrochemical workstation based on a conventional three-electrode system (a bare or modified GCE ($\Phi=4$ mm) as the working electrode, Ag/AgCl (saturated KCl) as the reference electrode, and a Pt wire as counter electrode). The ECL test was executed on a MPI-A multifunctional analyzer (Xi'An Remax Electronic Science & Technology Co. Ltd., Xi'An, China).

Native Polyacrylamide Gel Electrophoresis (PAGE).

The diverse samples were loaded on the notches filling with native polyacrylamide gel (16%) to perform electrophoresis in $1 \times$ TBE buffer at 120 V for 2 h. After dying with ethidium bromide (EB), the gel was photographed by the Bio-Rad Gel Doc XR+ System (Bio-Rad, U.S.A.).

Preparation of the Sample Solution.

First of all, 100 μ L of $1 \times$ CutSmart buffer including target miRNA-141 at different concentrations, Fc-H1 (2 μ M), Fc-H2 (2 μ M), and BbvI cleavage enzyme (0.08 U/ μ L) were incubated at 37 $^{\circ}$ C for 2 h in a centrifuge tube to execute the target cycling enzymatic amplification (TCEA), which produced two types of dsDNA labelled with Fc, respectively, (abbreviated as Fc-D1, Fc-D2) named as sample solution.

Fabrication of Biosensor.

Firstly, the TPE nanocrystals (NCs) were synthesized referring to our previous methods through desolvation method. [1] Before modification, the GCE ($\Phi = 4$ mm) was polished and rinsed as the previous method. [2] Then, 5 μ L of BSA-TPE NCs

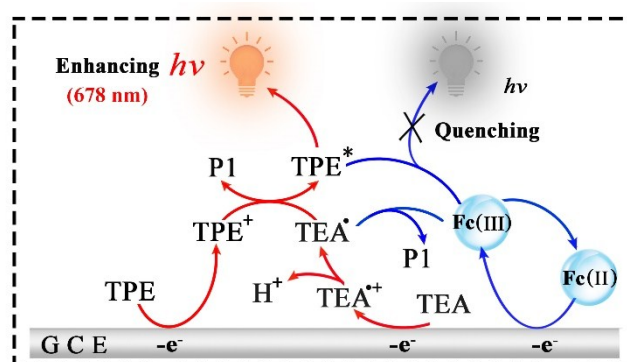
was coated on bare GCE to form a thin film. Subsequently, 10 μL of $\text{NH}_2\text{-}\beta\text{-CD}$ (1 mM) containing EDC and NHS (4:1) was dropped on the modified electrode to incubate overnight for cross-linking the $\text{NH}_2\text{-}\beta\text{-CD}$ and the BSA-TPE NCs containing abundant carboxy group (COOH). When the modified GCE was absolutely washed with deionized water, the functionalized electrode was reserved at 4 $^\circ\text{C}$. Then, 10 μL of BSA (0.25%) was incubated on the modified GCE for 40 min to seal the nonspecific binding sites. Subsequently, 10 μL of the sample solution were incubated on the modified GCE for 25 min. After rinsed with deionized water to eliminate the other materials, the ECL signal of the proposed biosensor was measured on the MPI-A multifunctional analyzer.

Measurement Procedure.

The proposed biosensor was measured at the potential from 0 to 1.6 V in 2 mL 0.1 M PBS (pH 7.4) containing 18 mM TEA with the voltage of the PMT high-voltage at 800 V.

Results and Discussion

The Possible ECL Mechanisms.



Scheme S1. The possible ECL enhancing mechanisms of BSA-TPE NCs/TEA system and ECL

quenching mechanisms of Fc.

ECL and EIS Characterization of the ECL Biosensing Platform.

The assembly steps of the sensing interface of the proposed biosensor were characterized by the ECL and EIS technique, respectively. In Fig. S1A, when the bare GCE was measured in detection solution by MPI-A ECL analyzer, nearly none ECL signal (curve a) was detected. However, the ECL signal of the BSA-TPE NCs modified GCE rose to 17230 a.u. (curve b) since the BSA-TPE NCs as ECL emitter reacted with the TEA. After the β -CD was assembled on GCE through the amide bond between the COOH of BSA and the NH_2 - β -CD, a slight reduction of ECL response (curve c) was recorded due to the obstruction of β -CD. As expected, the ECL signal (curve d) sequentially declined after the BSA was incubated on the electrode to insulate the nonspecific binding sites. Subsequently, when the sample solution containing plentiful of Fc-D1 and Fc-D2 were incubated on the modified electrode, the ECL signal obviously decreased (curve d) due to the quenching effect of Fc. Meanwhile, electrochemical impedance spectroscopy (EIS) characterizations of each steps were shown in Fig. S1B. Compared to the electron transfer resistance (R_{et}) of the bare GCE (curve a), the R_{et} of BSA-TPE NCs (curve b) was much larger, because of the blockade of the thin film on the electrode surface. After the β -CD was immobilized on the modified GCE successfully, the R_{et} (curve c) was decreased slightly, which ascribed to the formation of envelopes between the β -CD and the $[\text{Fe}(\text{CN})_6]^{3-/4-}$ to adsorb a small amount of $[\text{Fe}(\text{CN})_6]^{3-/4-}$ to the surface of GCE. Subsequently, the R_{et} values (curve d) slightly enlarged due to the insulation of BSA.

When the Fc-D1 and Fc-D2 entered the cavity of β -CD, the R_{et} values (curve e) were decreased rapidly. Thus, the EIS results were in accordance with the ECL analysis, illuminating the successful fabrication of the proposed biosensor.

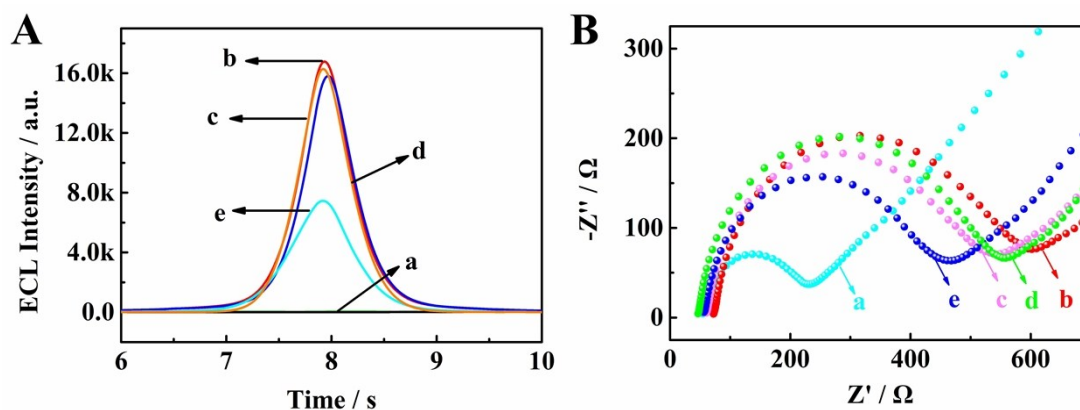


Fig. S1 (A) ECL characterization of the modified GCE in PBS containing 18 mM TEA and (B) EIS of the assembly steps of modified GCE in PBS (pH 7.4) containing 5.0 mM $[\text{Fe}(\text{CN})_6]^{3-/4-}$: (a) bare GCE, (b) BSA-TPE NCs/GCE, (c) β -CD/BSA-TPE NCs/GCE, (d) BSA/ β -CD/BSA-TPE NCs/GCE, (e) sample solution/BSA/ β -CD/BSA-TPE NCs/GCE.

Optimization of the Experimental Conditions.

Several optimizing experiments were performed to reach the excellent experimental performance. Firstly, the concentrations of two hairpins labeled with ferrocenes (Fc-H1, Fc-H2) was related to the sensitivity of the proposed biosensor. To obtain the optimal quenching efficiency, the concentrations of hairpins with 0.5 μM , 1.0 μM , 2.0 μM , 2.5 μM , 3.0 μM were employed to decrease the ECL signals. As revealed in Fig. S2A, descending ECL intensities were accordingly measured with the increase of hairpin due to the quenching of Fc. Finally, 2.0 μM was chosen as the optimal concentrations of hairpins. In the meantime, the reaction time of the target

cycling enzymatic amplification (TCEA) was also investigated. The ECL intensity declined dramatically as the reaction time increased (Fig. S2B), and the ECL signal remained essentially constant after 2 h. Thus, it indicated that the optimal reaction time of TCEA was 2 h at last. Furthermore, to demonstrate the efficient capability of host-guest molecular recognition, the bonding time between Fc and β -CD has been explored (Fig. S2C). Noticeably, the ECL responses dropped after the proposed biosensor was incubated with sample solution containing Fc-D1 and Fc-D2 with increasing time from 0 ~ 40 min. Finally, After the incubation time was greater than 25 min, the ECL intensity attained a relatively stable value because the Fc-D1 and Fc-D2 produced by TCEA were adsorbed into the β -CD totally. Thus, 25 min was chosen as the optimal bonding time.

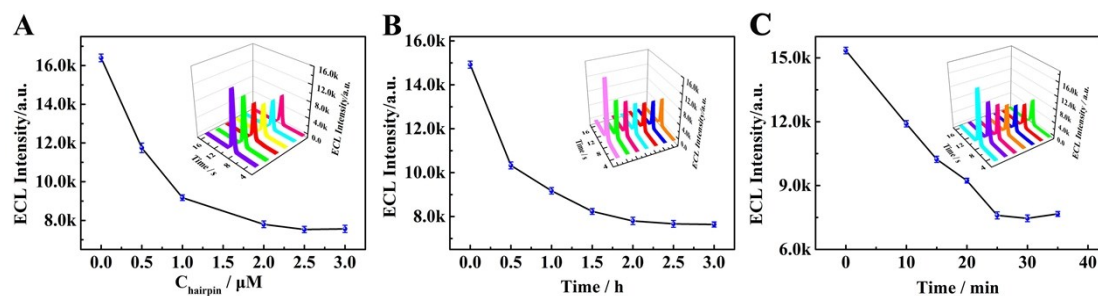


Fig. S2 (A) Optimum concentration of the hairpins, (B) Optimum reaction time of TCEA (with 100 fM miRNA-141), (C) Optimum bonding time between β -CD and Fc-D1, Fc-D2 (produced by TCEA with 100 fM miRNA-141).

The Sensitivity Analysis of the ECL Biosensing Platform.

Furthermore, to investigate the sensitivity of the proposed biosensors, the ECL responses of biosensors incubated with different sample solutions were executed. As exhibited in Fig. S3A, when the sample solution without target miRNA-141 were

incubated on the biosensor, a strong ECL signal (14920 a.u.) was observed, because of the wrong dimension matching between β -CD and two Fc on the hairpins, which cannot cause the degradation of ECL signal. Subsequently, the ECL response sharply dropped to 7954 a.u. (Fig. S3B) after the proposed biosensor interacted with sample solution containing Fc-D1 and Fc-D2 via the TCEA. The obvious decrease of ECL intensity was attributed to the highly efficient combination between β -CD and Fc, and close-range charge transport to the electrode surface. For comparison, we also investigated the sample solution in the absence of Bbv I to execute the target cycling amplification (TCA). As depicted in Fig. S3C, the ECL intensity (12887 a.u.) decreased slowly after the biosensor was incubated with sample solution containing Fc-H1-H2-Fc via the TCA. We speculated that the lengthy dsDNA of Fc-H1-H2-Fc blocked the hole of β -CD to prevent the further binding of Fc and β -CD when the Fc of Fc-H1-H2-Fc were bound to the electrode surface by molecular recognition, which reduced the molecular recognition efficiency. Therefore, we employed the TCEA with the aid of Bbv I to improve the sensitivity of the ECL biosensor.

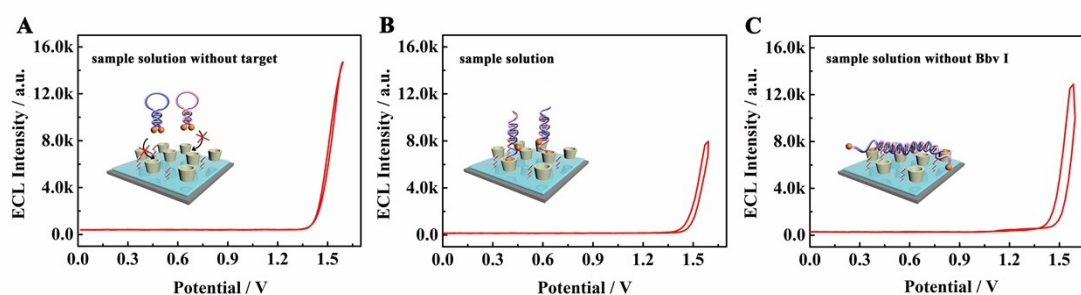


Fig. S3 The ECL intensities of the proposed biosensors incubated with (A) sample solution without target miRNA-141, (B) sample solution, (C) sample solution without BbvI.

Table. S2 Comparison for MiRNA Detection with Previous Methods.

method	target	detection limit	dynamic range	ref
CL RET	miRNA-141	0.28 pM	1 pM - 100 nM	3
DPV	miRNA-21	1.92 fM	5 pM - 0.5 fM	4
ECL	miRNA-141	0.4 fM	1.0 fM - 10 pM	5
ECL	miRNA-21	6.6 fM	10 fM - 0.1 nM	6
ECL	miRNA-141	13.6 aM	100 aM - 1 nM	this work

Performance of the proposed ECL biosensing platform.

To evaluate the performance of the developed ECL biosensor, the stability and selectivity of the proposed biosensor were investigated, respectively. The continuous scans over 13 cycles were measured to study the stability of the biosensor (with 100 fM miRNA-141) in the detection solution. As shown in Fig. S4A, the biosensor has shown no obvious undulation with a relative standard deviation (RSD) of 1.17% which demonstrated an excellent stability. Subsequently, miRNAs (miRNA-21, miRNA-199a, miRNA-155) as interferences were used to study the selectivity of the ECL biosensor for miRNA-141. According to Fig. S4B, the biosensor exhibited a significant ECL signal when the sample solution with no target (blank) was incubated on the biosensor, and the ECL intensities of miRNA-21 (10 pM), miRNA-199a (10 pM), and miRNA-155 (10 pM) did not show remarkable variation compared with the blank. Subsequently, the mixture [miRNA-141 (100 fM), miRNA-21 (10 pM), miRNA-199a (10 pM), and miRNA-155 (10 pM)] was measured by the proposed ECL biosensor. Compared with the ECL signal of individual miRNA-141 (100 fM), the ECL response of the mixture exhibited no obvious change, which indicated that the above interferences had barely no influence to the ECL signal of miRNA-141.

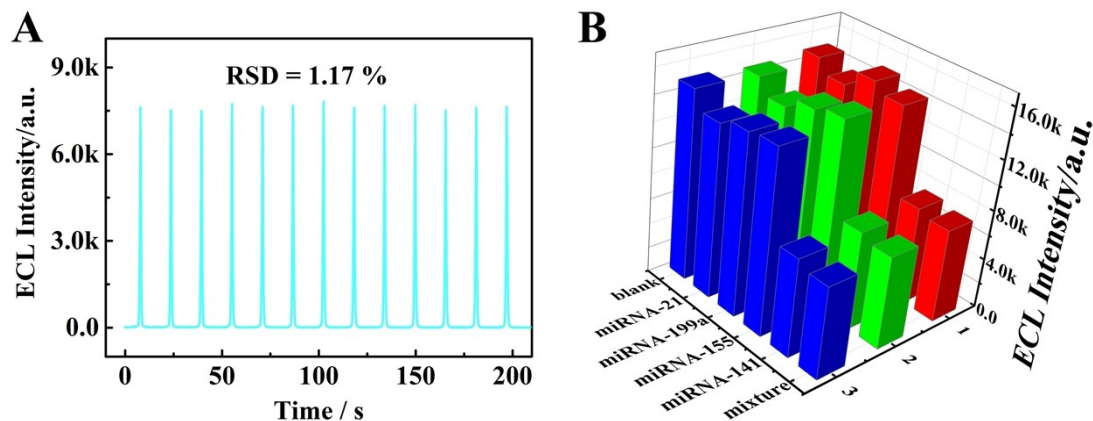


Fig. S4 (A) ECL stability of the biosensor by continuous scanning for 13 cycles in the presence of 100 fM miRNA-141. (B) Selectivity of the biosensor with target miRNA-141 (100 fM) and different interfering: miRNA-21 (10 pM), miRNA-199a (10 pM), miRNA-155 (10 pM) and mixture solution (miRNA-141, miRNA-21, miRNA-199a, miRNA-155).

The method of LOD calculation.

We calculated the LOD employing the traditional and typical approach reported in the previous references [7-8]. An ECL measurement for blank samples was executed with three parallel tests, which exhibited average ECL intensity of 14750 a.u. with standard deviation (S_B) of 191.8. To calculate the LOD, with signal-to-noise ratio value (k_1) of 3, the changes in the ECL intensities (ΔI_{ECL}) were found to be linearly depended on the logarithm of miRNA-141 concentration, so the $I_B = 0$, the smallest detectable signal could be calculated as

$$IL = I_B + k_1 S_B = 575.4$$

According to the linear regression equation $\Delta I_{ECL} = 13312.6 + 1619.05 \lg c$, the LOD could be calculated as 13.6 aM.

Application of the biosensor in tumor cells.

To assess the capacity of the developed biosensor in cancer cell, the lysates of human breast cancer cell MDA-MB-231 were applied to execute an ECL assay with number of cell from 10^0 to 10^6 cells. As revealed in Fig. S5, the correction coefficient of 0.997 was achieved from the regression curve (red x-axis), displaying a good linear correlation. Compared to the calibration curve of standard samples (blue x-axis), the calibration curve for actual tumor cell samples possessed an approximate slope, which demonstrated that the proposed biosensor has a satisfactory adaptability for practical samples.

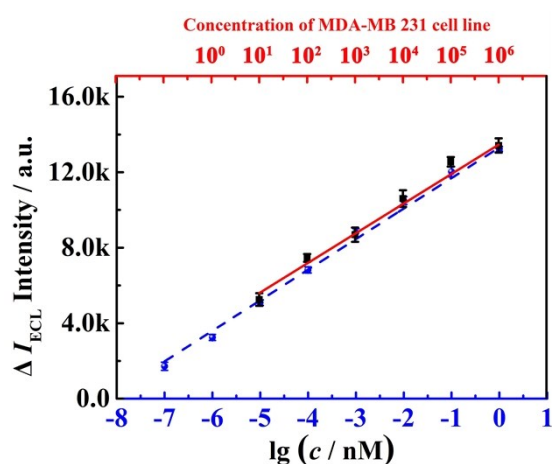


Fig. S5 The application of the proposed biosensor in the MDA-MB-231 cell line (red line), and the calibration curve of standard miRNA-141 assay (blue line).

References

- 1 J. L. Liu, J. Q. Zhang, Z. L. Tang, Y. Zhuo, Y. Q. Chai, R. Yuan, *Chem. Sci.*, 2019, **10**, 4497.
- 2 J. H. Luo, D. Cheng, P. X. Li, Y. Yao, S. H. Chen, R. Yuan, W. J. Xu, *Chem. Commun.*, 2018, **54**, 2777.
- 3 A. F. Jou, C. H. Lu, Y. C. Ou, S. S. Wang, S. L. Hsu, I. Willner, J. A. Ho, *Chem. Sci.*, 2015, **6**, 659.
- 4 L. Cui, M. Wang, B. Sun, S. Y. Ai, S. C. Wang, C. Y. Zhang, *Chem. Commun.*, 2019, **55**, 1172.

- 5 H. J. Lu, J. B. Pan, Y. Z. Wang, S. Y. Ji, W. Zhao, X. L. Luo, J. J. Xu, H. Y. Chen. *Anal. Chem.*, 2018, **90**, 10434.
- 6 P. Zhang, J. Jiang, Ruo. Yuan, Y. Zhuo, Y. Q. Chai, *J. Am. Chem. Soc.*, 2018, **140**, 9361.
- 7 G. Long, J. D. Winefordner, *Anal. Chem.*, 1983, **55**, 712A.
- 8 V. A. Zamolo, G. Valenti, E. Venturelli, O. Chaloin, M. Marcaccio, S. Boscolo, M. Poli, *ACS nano*. 2012, **6**, 7989.